# Supplementary Materials: Climate Change Impacts on US Water Quality Using Two Models: HAWQS and US Basins

**Charles Fant, Raghavan Srinivasan, Brent Boehlert, Lisa Rennels, Steven C. Chapra, Kenneth M. Strzepek, Joel Corona, Ashley Allen and Jeremy Martinich**

## Rationale for Selection of Climate Models

As in most impacts work, the selection of a subset of general circulation models (GCMs) is necessary due to computational, time, and resource constraints. As such, five GCMs were chosen with the intent of ensuring that the subset captures a large range of the variability in climate outcomes observed across the entire ensemble from the fifth phase of the Coupled Model Intercomparison Project (CMIP5; Taylor et al. 2012).

| Center (Modeling Group) | Model Acronym | Availability | | References |
|---|---|---|---|---|
| | | LOCA | SNAP | |
| National Center for Atmospheric Research | CCSM4 | X | X | Gent et al. 2011; Neale et al. 2013 |
| NASA Goddard Institute for Space Studies | GISS-E2-R | X | X | Schmidt et al. 2006 |
| Canadian Centre for Climate Modeling and Analysis | CanESM2 | X | | Von Salzen et al. 2013 |
| Met Office Hadley Centre | HadGEM2-ES | X | | Collins et al., 2011; Davies et al. 2005 |
| Atmosphere and Ocean Research Institute, National Institute for Environmental Studies, and Japan Agency for Marine-Earth Science and Technology | MIROC5 | X | | Watanabe et al. 2010 |

<u>Variability in Climate Outcomes</u>

While many different metrics could be used in this type of comparison, a logical approach is to compare the projections from CMIP5 CGMs for annual and seasonal temperature and precipitation. While these averaged metrics may not be perfect substitutes for comparing extreme weather effects, the relationship should be sufficiently strong for selecting climate models from the broader ensemble.

The following scatter plots[1] show the variability across the CMIP5 ensemble for projected changes (2071-2100 compared to 1976-2005 baseline) in annual and seasonal (primarily summertime) temperature and precipitation.[2]

[1] These scatter plots were developed using the LASSO tool, a product of EPA's Office of Research and Development – National Center for Environmental Assessment.

[2] A number of the GCMs in the plots contain multiple initializations that are designed with numbers in subscript. The dashed lines represent the median value for each axis.

**Figure 1.** Variability of projected annual temperature and precipitation change across the CMIP5 ensemble for the contiguous US

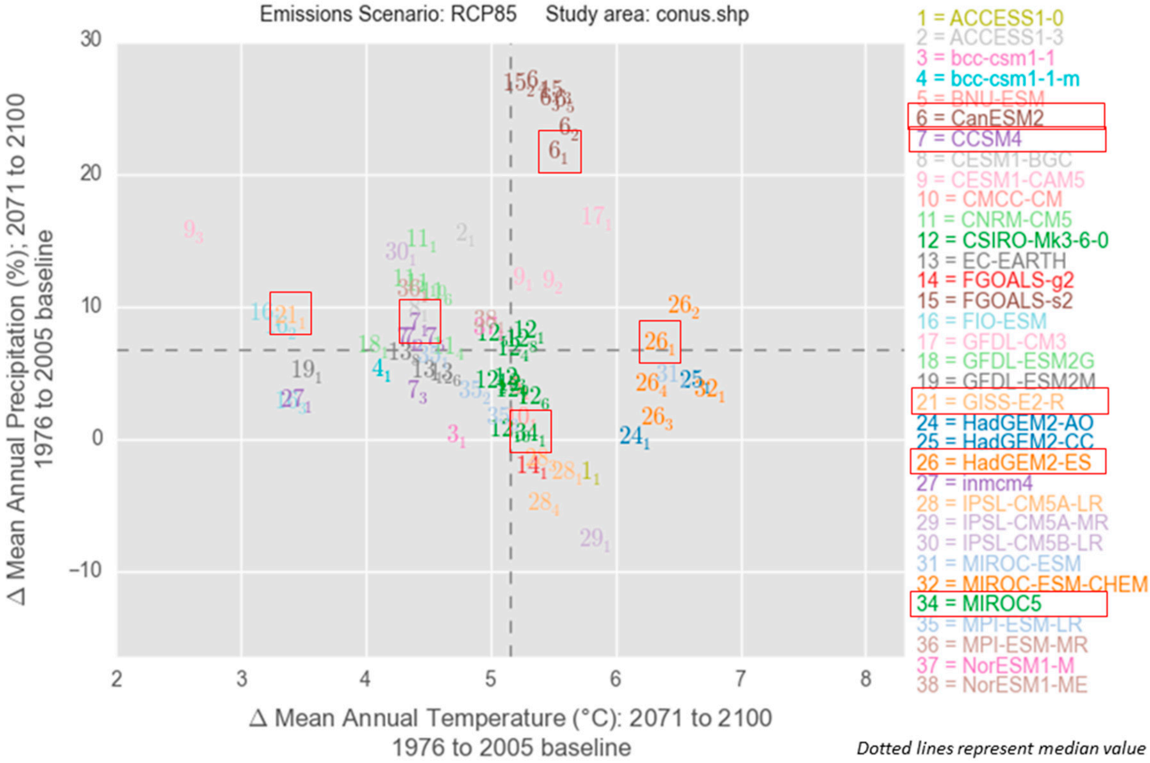


**Figure 2.** Variability of projected summertime temperature and precipitation change across the CMIP5 ensemble for the contiguous US

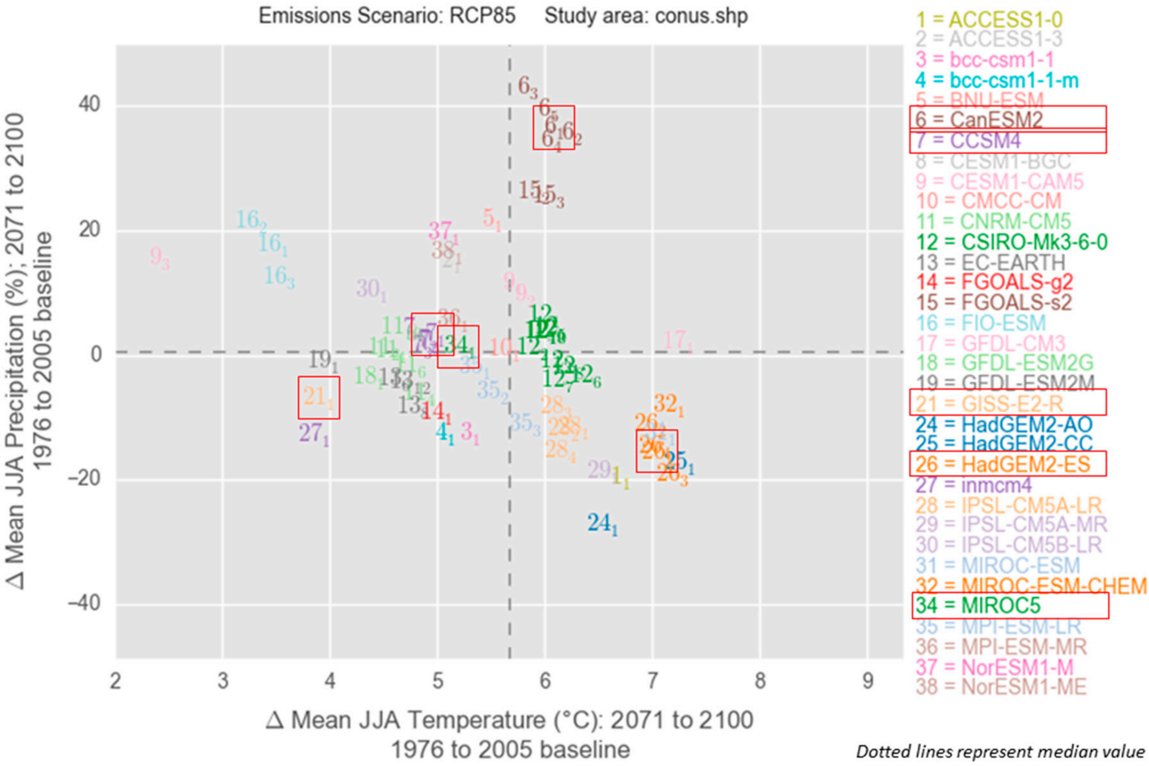


**Figure 3.** Variability of projected wintertime temperature and precipitation change across the CMIP5 ensemble for the contiguous US

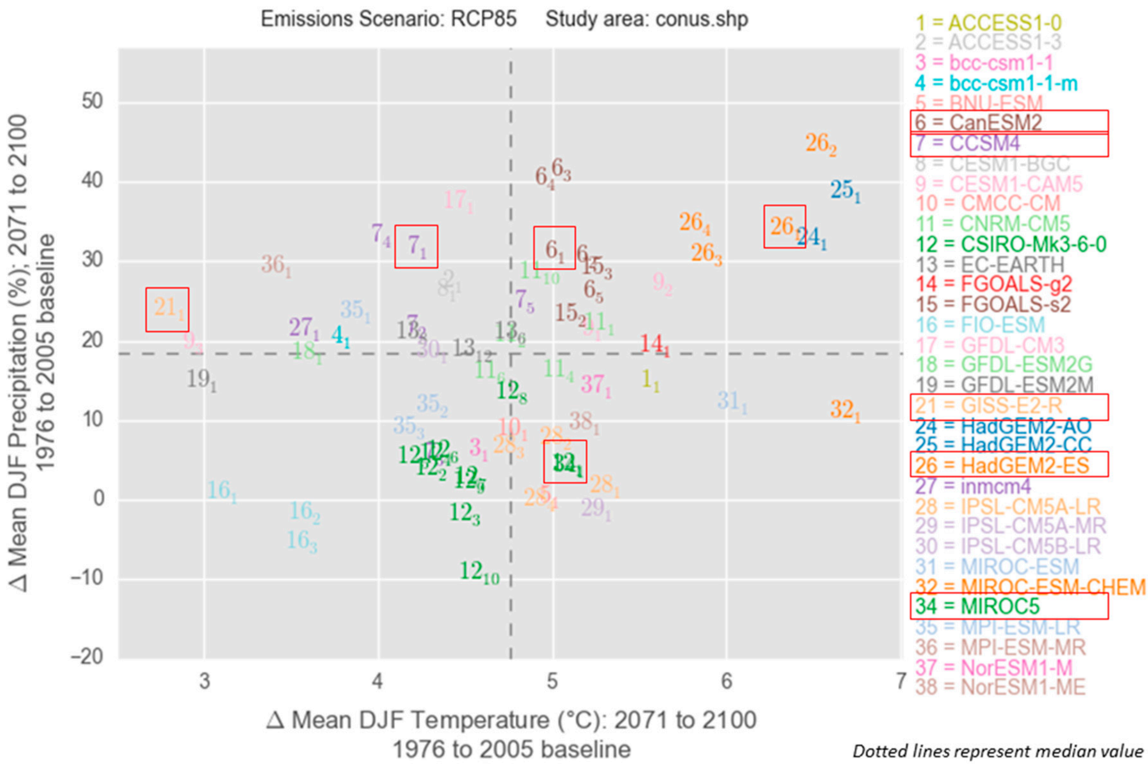


As shown in Figures 1-3, the five selected GCMs (CanESM2, CCSM4, GISS-E2-R, HadGEM2-ES, and MIROC5) cover a large range of the variability across the entire ensemble in terms of annual and season temperature and precipitation. This selection also balances the range alongside considerations of model independence, broader usage by the scientific community, and skill at reproducing observed climate. Sanderson et al. (2015a, 2015b) provide analysis of both model skill at the global scale and independence of underlying code. These criteria were considered in the selection process.

**References**


Collins WJ, Bellouin N, Doutriaux-Boucher M, Gedney N, Halloran P, Hinton T, Hughes J, Jones CD, Joshi M, Liddicoat S, Martin G. 2011. Development and evaluation of an Earthsystem model–HadGEM2. Geoscience Model Develeopment, 4:1051-1075.

Davies T, Cullen MJ, Malcolm AJ, Mawson MH, Staniforth A, White AA, Wood N. 2005. A new dynamical core for the Met Office's global and regional modelling of the atmosphere. Quarterly Journal of the Royal Meteorological Society, 131:1759-1782.

Gent PR, Danabasoglu G, Donner LJ, Holland MM, Hunke E, Jayne S, Lawrence D, Neale RB, Rasch PJ, Vertenstein M, Worley PH. 2011. The community climate system model version 4. Journal of Climate, 24:4973-4991.

Neale RB, Richter J, Park S, Lauritzen PH, Vavrus SJ, Rasch P, Zhang M. 2013. The mean climate of the community Atmosphere Model (CAM4) in forced SST and fully coupled experiments. Journal of Climate, 26:5150-5168.

Sanderson B, Knutti R, Caldwell P (2015) A representative democracy to reduce interdependency in a multimodel ensemble. Journal of Climate. doi: 10.1175/JCLI-D-14-00362.1

Sanderson B, Knutti R, Caldwell P (2015) Addressing interdependency in a multi-model ensemble by interpolation of model properties. Journal of Climate. doi: 10.1175/JCLI-D-14-00361.1

Schmidt GA, Ruedy R, Hansen JE, Aleinov I, Bell N, Bauer M, Bauer S, Cairns B, Canuto V, Cheng Y, Del Genio A. 2006. Present-day atmospheric simulations using GISS ModelE: Comparison to in situ, satellite, and reanalysis data. Journal of Climate, 19:153-192.

Taylor KE, Stouffer RJ, Meehl GA (2012) An overview of CMIP5 and the experiment design. Bulletin of the American Meteorological Society. doi:10.1175/BAMS-D-11-00094.1

von Salzen K, Scinocca JF, McFarlane NA, Li J, Cole JN, Plummer D, Verseghy D, Reader MC, Ma X, Lazare M, Solheim L. 2013. The Canadian fourth generation atmospheric global climate model (CanAM4). Part I: representation of physical processes. Atmosphere-Ocean, 51:104-125.

Watanabe M, Suzuki T, O'ishi R, Komuro Y, Watanabe S, Emori S, Takemura T, Chikira M, Ogura T, Sekiguchi M, Takata K. 2010. Improved climate simulation by MIROC5: mean states, variability, and climate sensitivity. Journal of Climate 23:6312-6335.

**Calculation of the Climate-oriented Water Quality Index (CWQI)**

As mentioned in the manuscript, calculation of the Climate-oriented Water Quality Index (CWQI) involves three major steps:

1. Obtain measurements on water quality constituents, obtained directly from the water quality models,
2. Convert each measurement into a subindex using water quality curves and
3. Aggregate the subindex values into the WQI.

Step #1 involves post-processing of the water quality model outputs on a daily basis. These outputs were aggregated the Level-III Ecoregions, as was done in EPA (2015). Step #2 is the most involved and uses four subindex calculations: Concentrations of total phosphorus, total nitrogen, and DO, as well as water temperature. These are described below

<u>Total Phosphorus subindex calculation</u>

This is based on EPA (2015). The subindex ($SI_{TP}$) is calculated as follows:

$$SI_{TP} = 10, \quad when\ TP > TP_{10}$$
$$SI_{TP} = a * \exp(TP * b), \quad when\ TP_{100} < TP \leq TP_{10}$$
$$SI_{TP} = 100, \quad when\ TP \leq TP_{100}$$

Where TP is total phosphorus concentration in the Eco Region, $TP_{10}$, $TP_{100}$, a, and b are all region-specific parameters listed in EPA (2015).

<u>Total Nitrogen subindex calculation</u>

This is based on EPA (2015). The subindex ($SI_{TN}$) is calculated as follows:

$$SI_{TN} = 10, \quad when\ TN > TN_{10}$$
$$SI_{TN} = a * \exp(TN * b), \quad when\ TN_{100} < TN \leq TN_{10}$$
$$SI_{TN} = 100, \quad when\ TN \leq TN_{100}$$

Where TN is total nitrogen concentration in the Eco Region, $TN_{10}$, $TN_{100}$, a, and b are all region-specific parameters listed in EPA (2015).

<u>DO subindex calculation</u>

This is based on EPA (2015) but does not vary by region. The subindex ($SI_{DO}$) is calculated as follows:

$$SI_{DO} = 10, \quad when\ DO \leq 3.3\ mg/L\ and\ DO\ saturation \leq 100\%$$
$$SI_{DO} = -80.29 + 31.88 * DO - 1.401 * DO^2, \quad when\ 3.3\ mg/L < DO \leq 10.5\ mg/L\ and\ DO\ saturation \leq 100\%$$
$$SI_{DO} = 100, \quad when\ DO \geq 10.5\ mg/L\ and\ DO\ saturation \leq 100\%$$
$$SI_{DO} = 100 * \exp\big((DOsat - 100) * -1.197 * 10^{-2}\big), \quad when\ 100\% < DOsat \leq 275\%$$
$$SI_{DO} = 10, \quad when\ DOsat \geq 275\%$$

Where DO is Dissolved Oxygen, DOsat is DO saturation.

<u>Water Temperature subindex calculation</u>

This is based on the method and subindex curve from McClelland (1974), which uses deviations from an average seasonal water temperature and is penalized if temperatures are either higher or lower than average. More details on this can be found in McClelland (1974) as well as Boehlert (2015), where the same method is used. The subindex curve was not accompanied by an equation, so this has been replicated by the authors using a polynomial fit. The equations used are as follows:

$$SI_T = 0.0021 * \Delta T^3 + 0.4339 * \Delta T^2 - 12.826 * \Delta T + 98.41, \quad when\ 15 \geq \Delta T > 0$$
$$SI_T = 0.1789 * \Delta T^3 + 0.0885 * \Delta T^2 - 3.9366 * \Delta T + 92.07, \quad when - 15 \leq \Delta T \leq 0$$
$$SI_T = 5, \quad when\ \Delta T > 15\ or\ \Delta T < -15$$

Where $\Delta T$ is the change in seasonal mean temperature.

Climate Oriented Water Quality Index

The four subindices are aggregated using the weights listed in McClelland (1974), which are rescaled to sum to one such that the DO subindex weight becomes 0.36 and the other three become 0.21. The final value of the is calculated using an arithmetic weighted average of the four subindices.

**References**

Boehlert, B.; Strzepek, K. M.; Chapra, S. C.; Fant, C.; Gebretsadik, Y.; Lickley, M.; Swanson, R.; McCluskey, A.; Neumann, J.; Martinich, J. Climate change impacts and greenhouse gas mitigation effects on US water quality. Journal of Advances in Modeling Earth Systems, **2015**, 7(3), 1326-1338.

McClelland, N. I.; Water quality index application in the Kansas River Basin, prepared for the U.S. Environmental Protection Agency—Region 7, EPA-907/9-74-001, **1974**.

United States Environmental Protection Agency Office of Water. Benefit and Cost Analysis for the Effluent Limitation Guidelines and Standards for the Steam Electric Power Generating Point Source Category. EPA-821-R-15-005. 2015. Available online: https://www.epa.gov/eg/steam-electric-power-generating-effluent-guidelines-2015-final-rule-documents (accessed on 15 November, 2016).

## Maps of Future Changes in Air Temperature, Precipitation, Non-point Loadings, Flow, Water Temperature, Dissolved Oxygen, Total Nitrogen, Total Phosphorus, CWQI, and WTP for all five GCMs

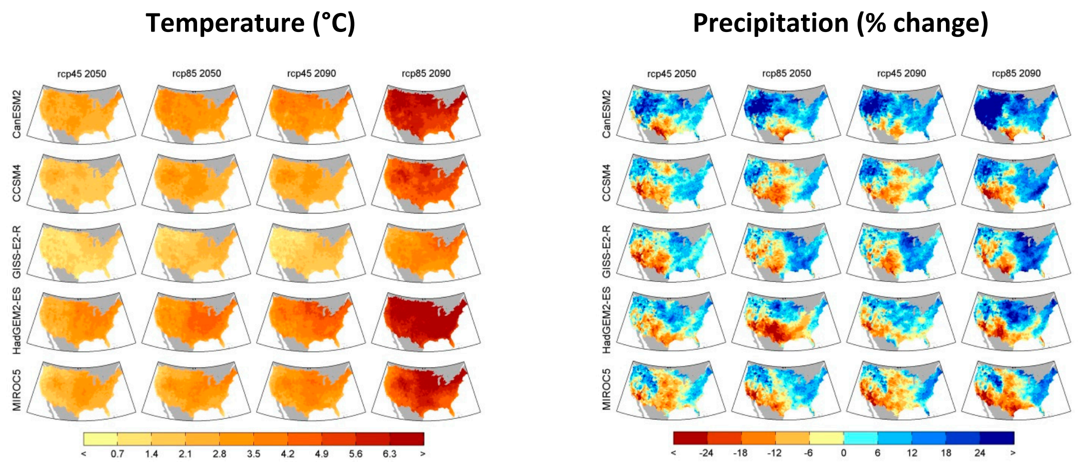


**Figure 1: Mean projected changes in temperature (°C; left) and precipitation (%; right) for the five climate models, two emissions scenarios, and the 2050 and 2090 eras. Changes are between the average of the 20-year projected era and the 20-year baseline.**

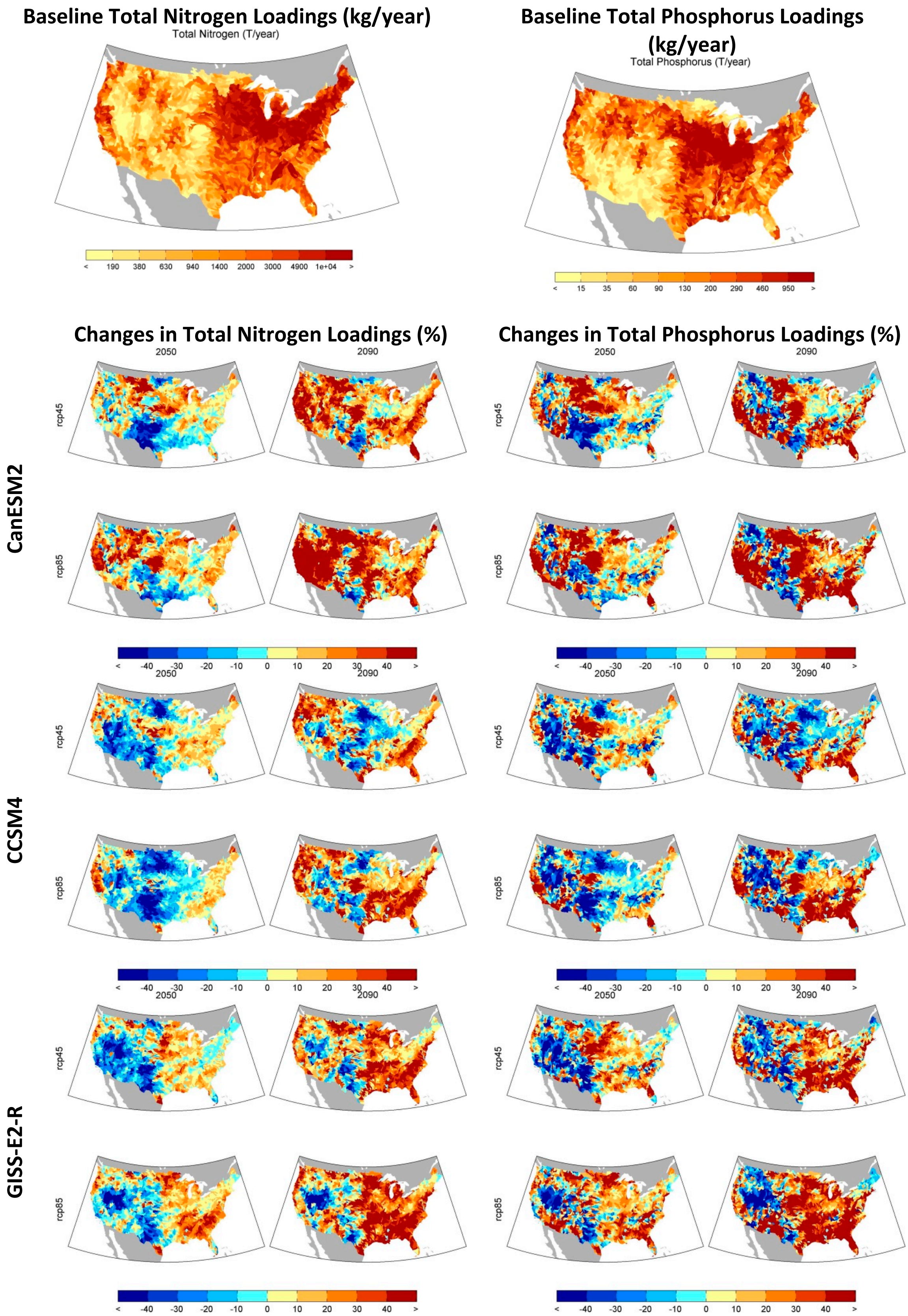
Baseline Total Nitrogen Loadings (kg/year)
Total Nitrogen (T/year)
< 190 380 630 940 1400 2000 3000 4900 1e+04 >
Baseline Total Phosphorus Loadings (kg/year)
Total Phosphorus (T/year)
< 15 35 60 90 130 200 290 460 950 >
Changes in Total Nitrogen Loadings (%)
Changes in Total Phosphorus Loadings (%)
2050
2090
rcp45
rcp85
CanESM2
CCSM4
GISS-E2-R
< -40 -30 -20 -10 0 10 20 30 40 >

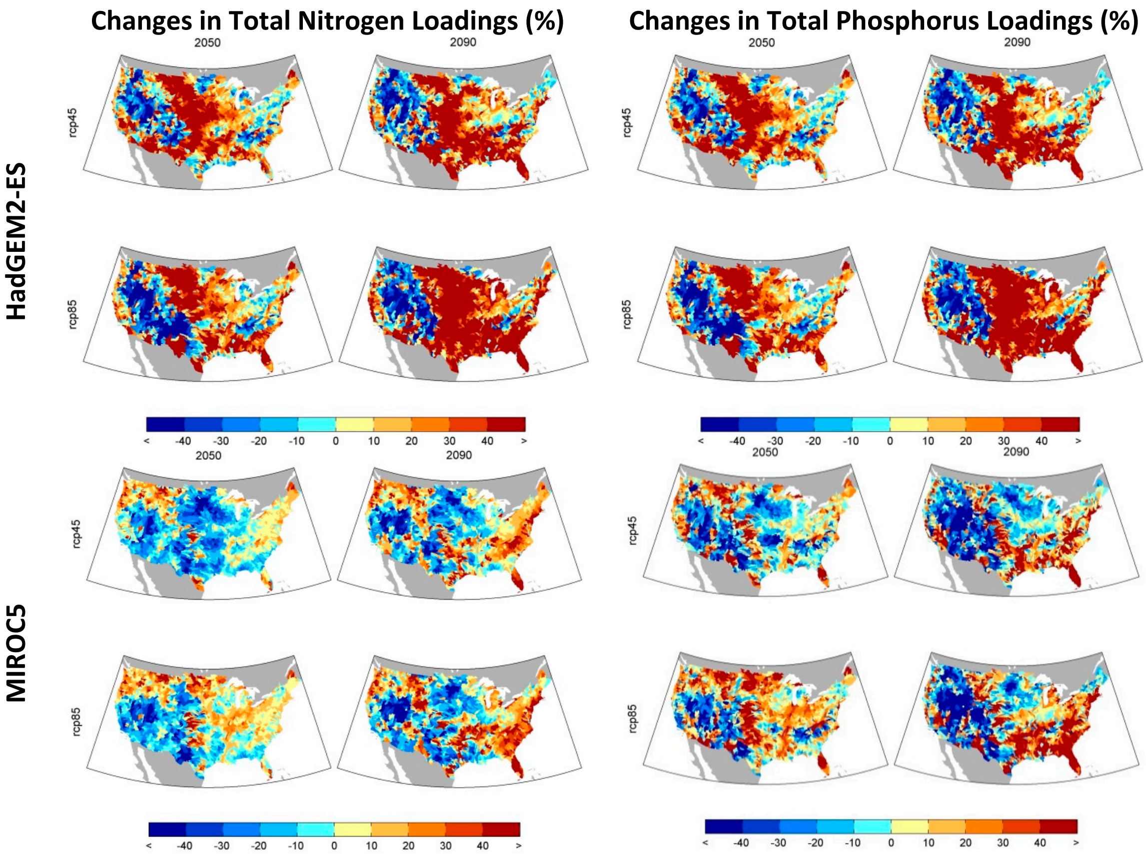


**Figure 2: Non-point source nitrogen and phosphorus agricultural loadings under the baseline (top) and climate change (bottom) derived from HAWQS outputs. Variability in loading patterns across climate scenarios, emissions scenarios, and time is driven by the response of the landscape model to changes in river runoff under climate change.**

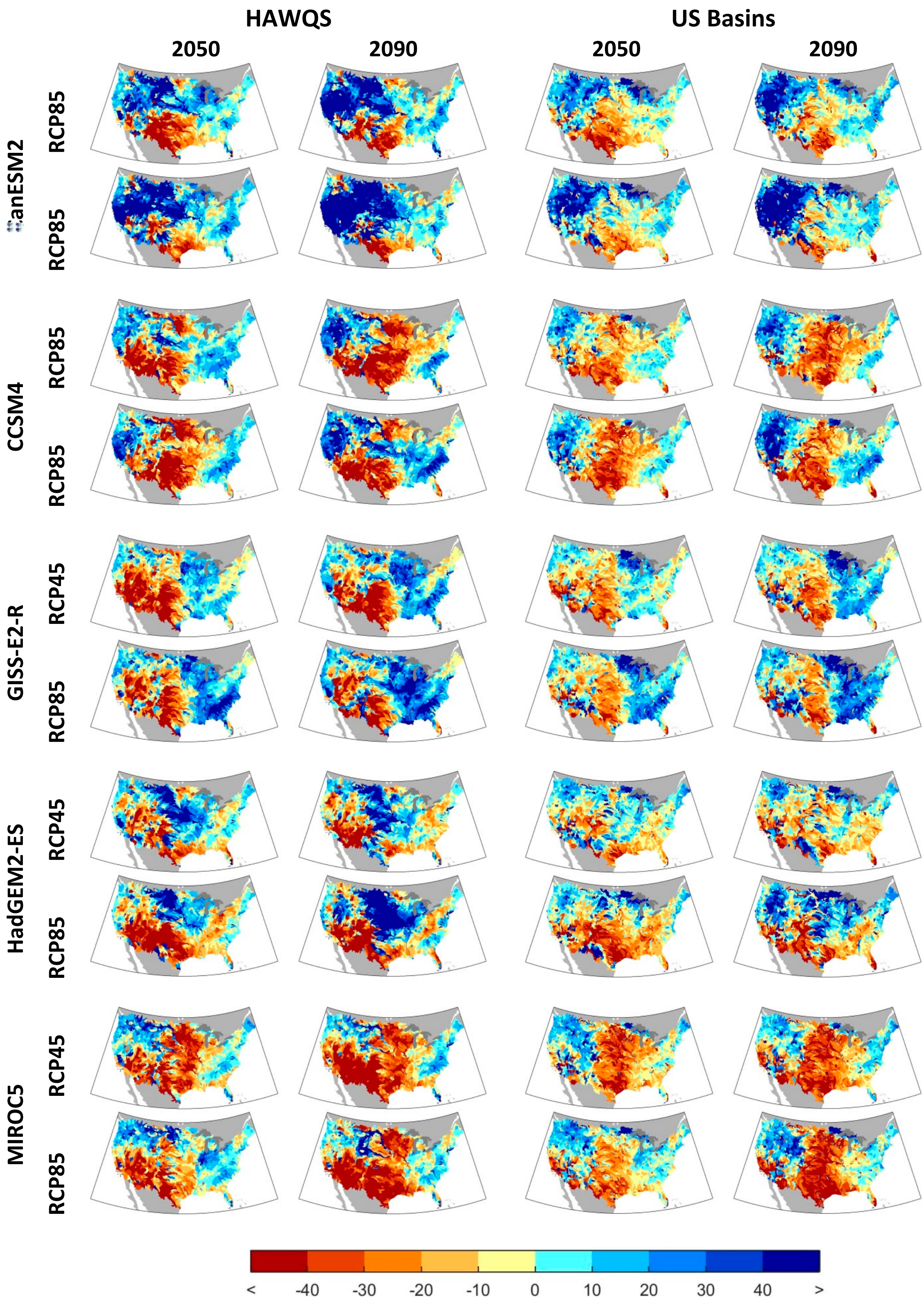


**Figure 3: Percentage changes in mean projected HAWQS and US Basins river flow for both the GISS-E2-R and MIROC5 climate models, two emissions scenarios, and two eras.**

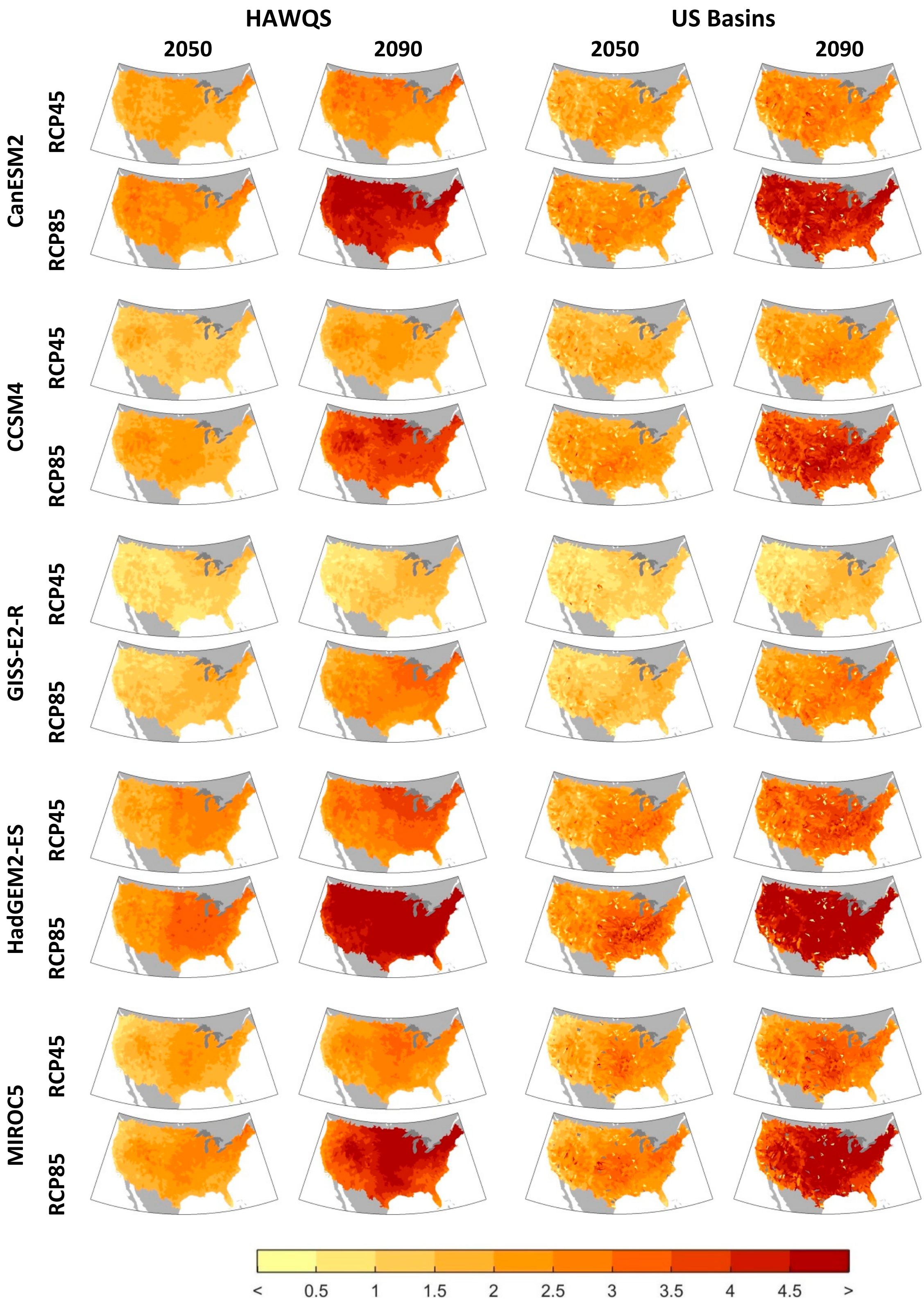


**Figure 4: Changes (°C) in mean projected HAWQS and US Basins water temperature for both the GISS-E2-R and MIROC5 climate models, two emissions scenarios, and two eras.**

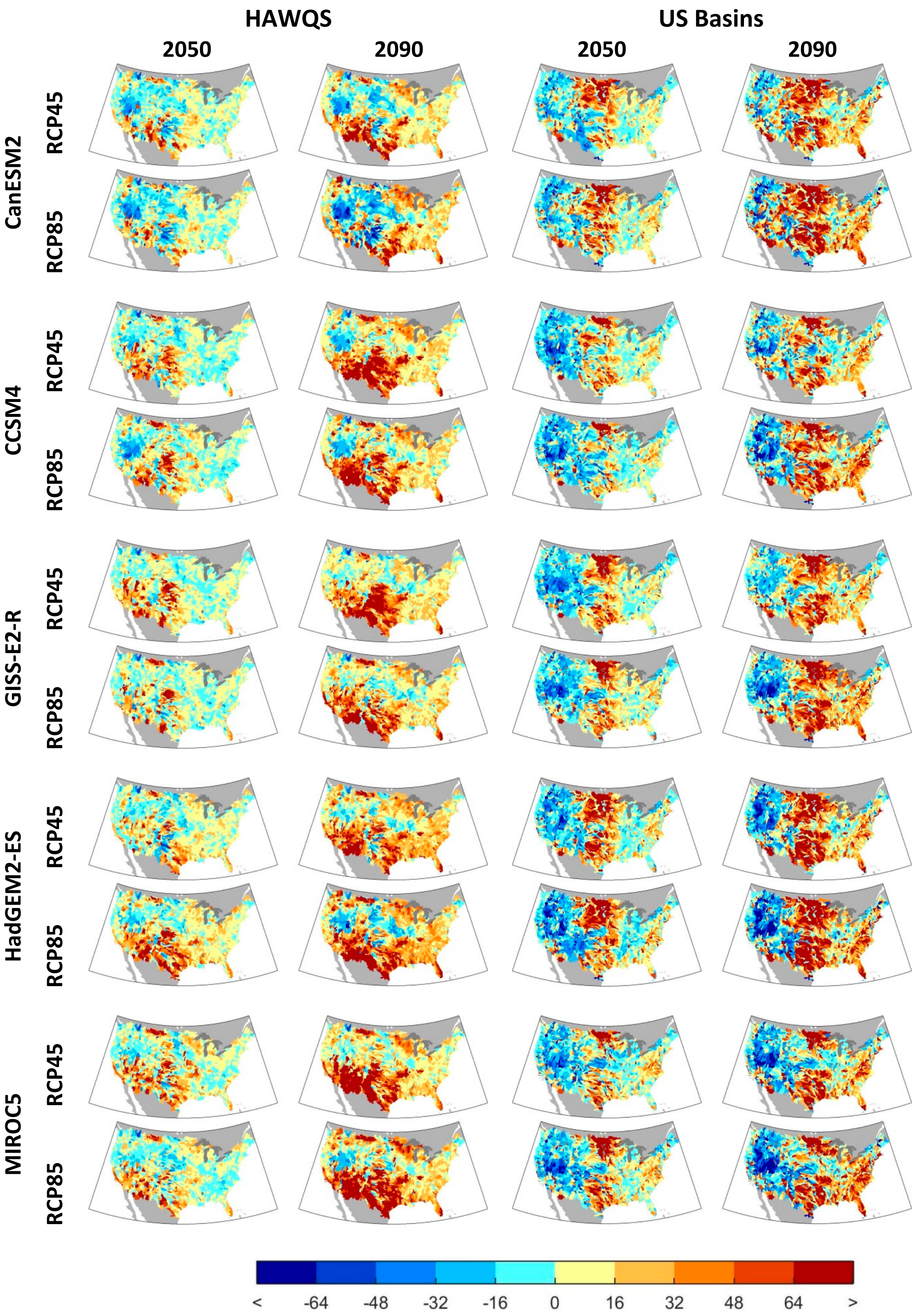


**Figure 5: Percentage changes in mean HAWQS and US Basins nitrogen concentrations for both the GISS-E2-R and MIROC5 climate models, two emissions scenarios, and two eras.**

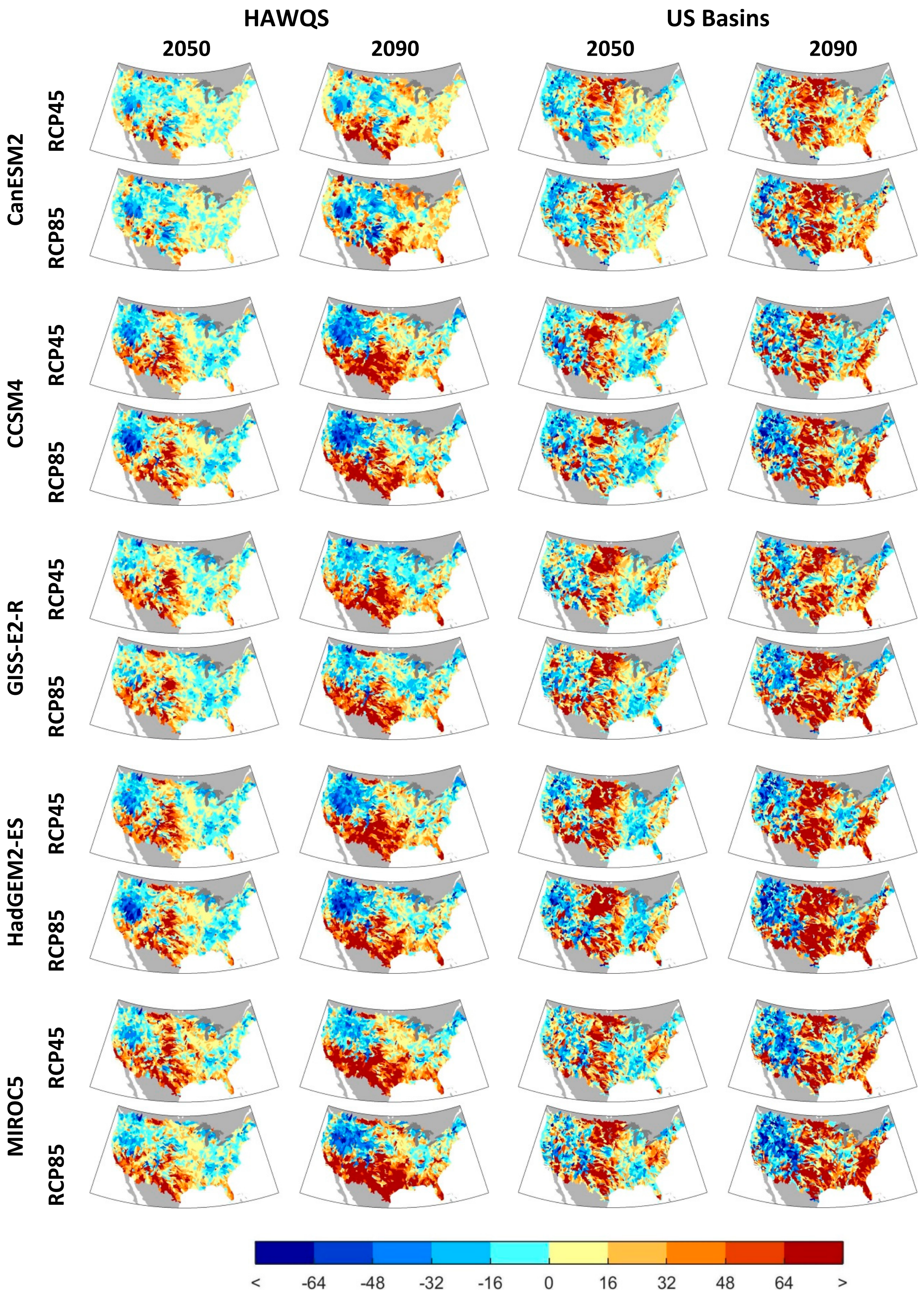


**Figure 6: Percentage changes in mean HAWQS and US Basins phosphorus concentrations for both the GISS-E2-R and MIROC5 climate models, two emissions scenarios, and two eras.**

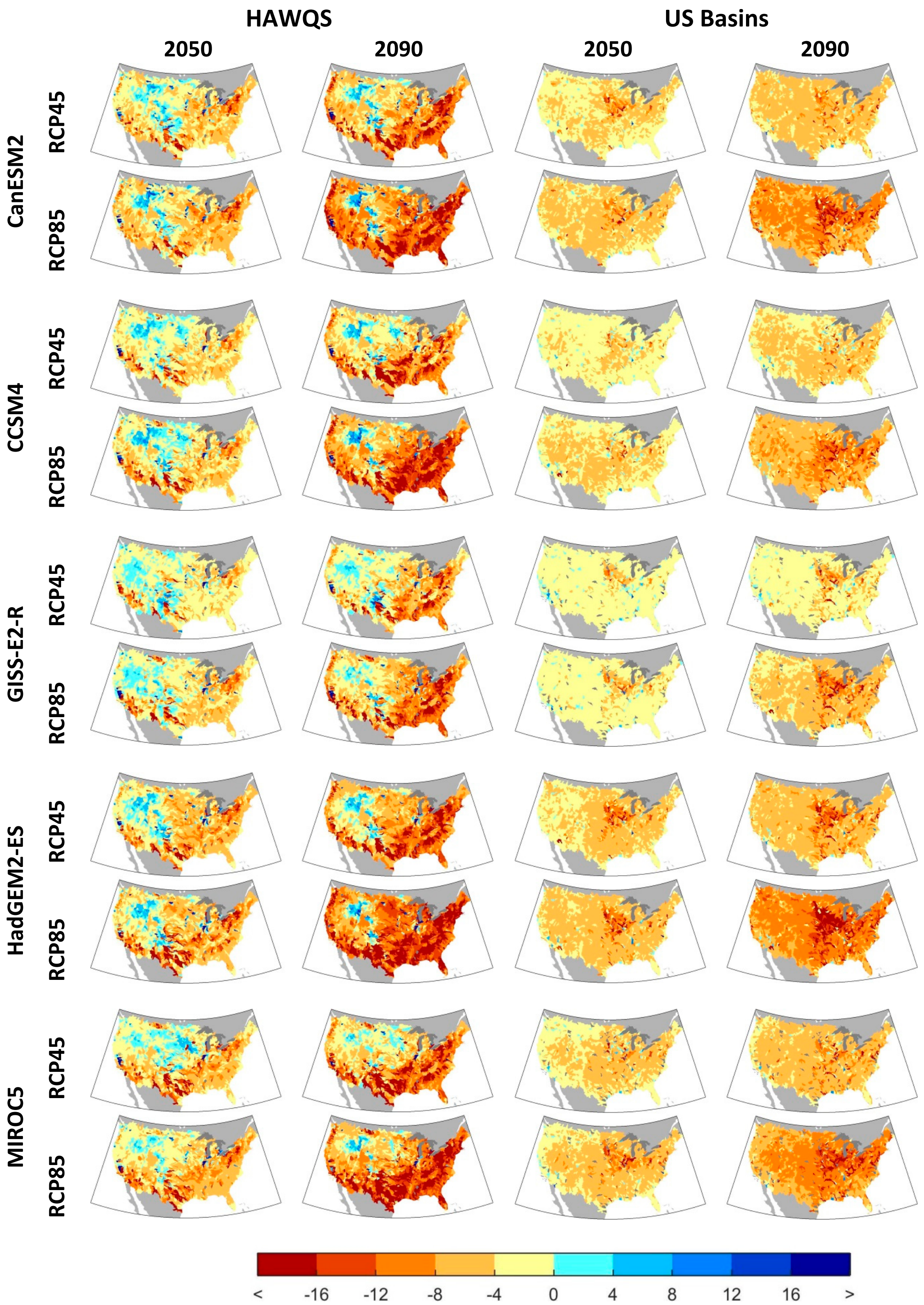


**Figure 7: Percentage changes in mean HAWQS and US Basins dissolved oxygen for both the GISS-E2-R and MIROC5 climate models, two emissions scenarios, and two eras.**

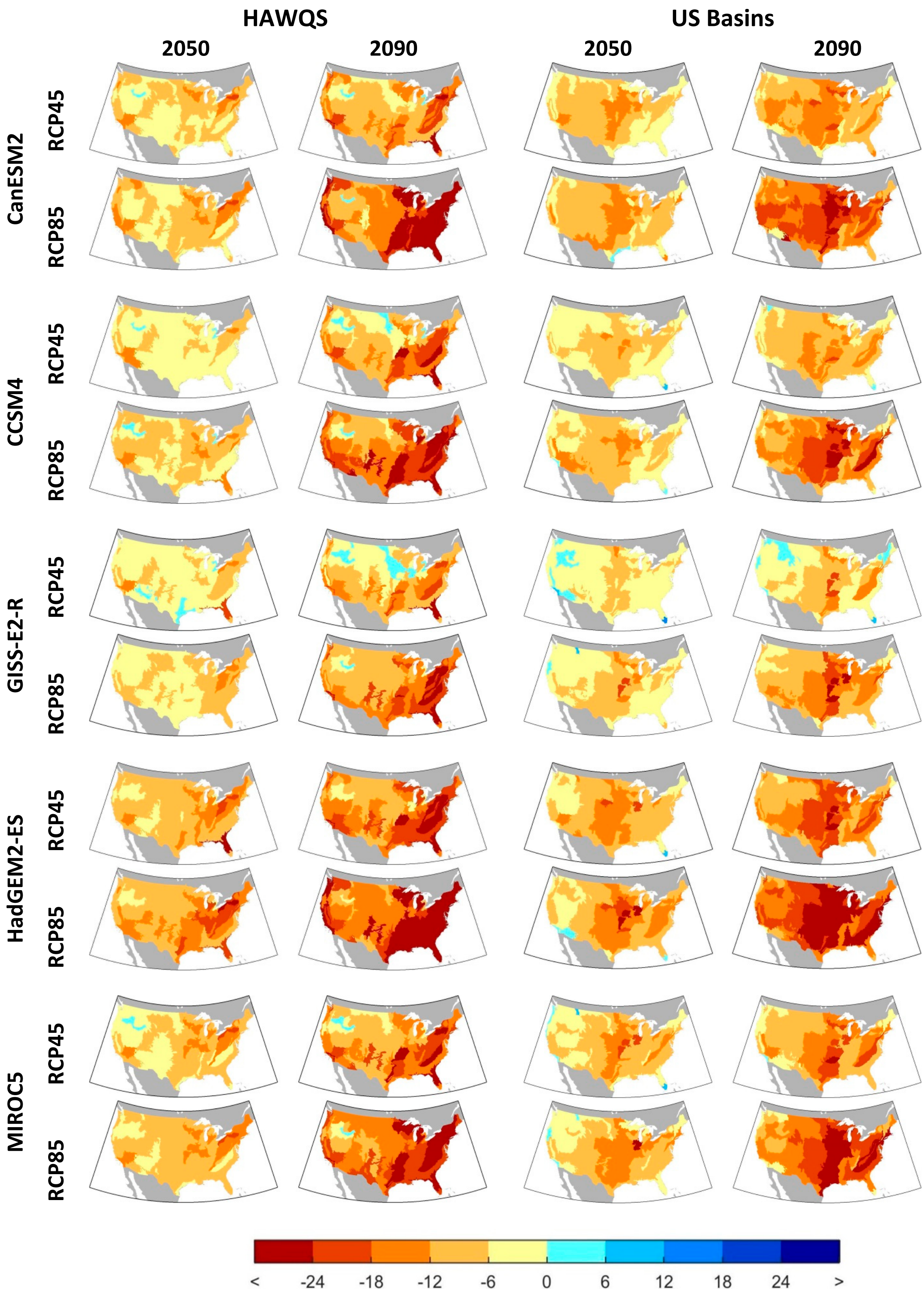


**Figure 8: Changes in mean HAWQS and US Basins levels of the Climate-Water Quality Index for both the GISS-E2-R and MIROC5 climate models, two emissions scenarios, and two eras.**

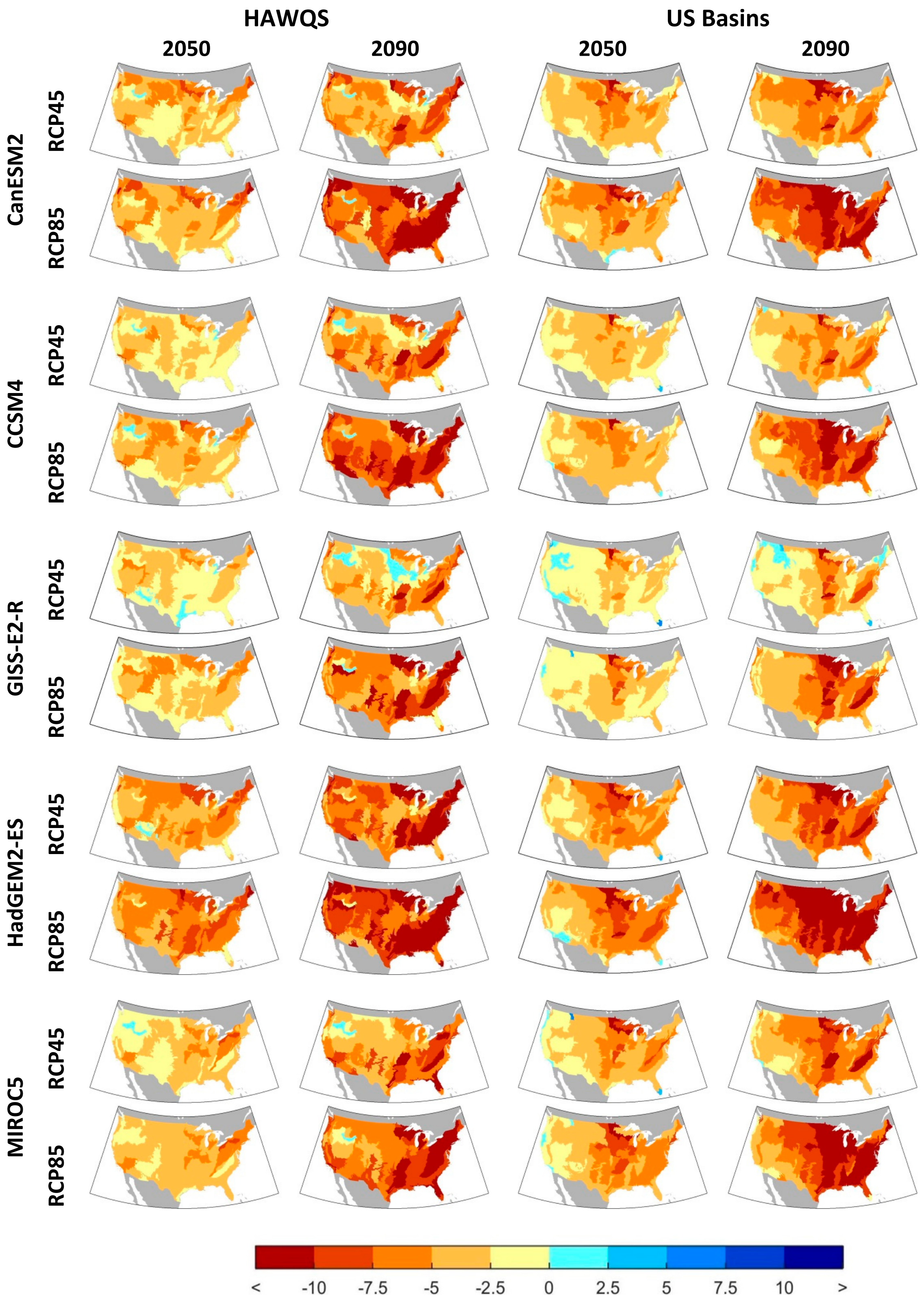


**Figure 9: Changes in mean HAWQS and US Basins Willingness To Pay per person (USD/year) for both the GISS-E2-R and MIROC5 climate models, two emissions scenarios, and two eras.**